ELECTROCHEMICAL PROPERTIES OF 2,6-BIS((E)-2-(FURAN-2-YL) VINYL)-4-(AZULEN-1-YL) PYRIDINE

Oana Iulia ENACHE [1], Ovidiu-Teodor MATICA [2], Magdalena-Rodica BUJDUVEANU [3], Eleonora-Mihaela UNGUREANU[4], Mihaela CRISTEA [5]

*The electrochemical study of 2,6-bis((E)-2-(furan-2-yl)vinyl)-4-(azulen-1-yl) pyridine (**L**) was performed on glassy carbon working electrode by using cyclic voltammetry (CV), differential pulse voltammetry (DPV), and rotating disk electrode voltammetry (RDE). The CV, DPV and RDE curves for **L** were recorded at its different concentrations in 0.1M TBAP/ CH_3CN non-aqueous solution. The CV curves were also recorded at variable scan rates and on precise domains of potential to estimate the degree of reversibility of the evidenced processes. Polymeric films were formed by electrochemical oxidation either by cycling the potential in the anodic scans or by controlled potential electrolysis at different anodic potentials and charges. The obtained modified electrodes were tested as sensors for heavy metal ions.*

Keywords: 2,6-bis((E)-2-(furan-2-yl) vinyl)-4-(azulen-1-yl)pyridine, cyclic voltammetry, differential pulse voltammetry, rotating disk voltammetry, chemically modified electrodes, heavy metal ions detection

1. Introduction

Azulene derivatives which were less or more grafted with various heterocycles were previously investigated by electrochemical methods to establish their ability to recognize heavy metal (HM) ions for analytical purposes, such as sensors [1-3]. Polymerization systems based on polyaniline, polyrhodanine, polypyrrole and polythiophene have been extensively studied for various applications due to their electrical conductivity and remarkable thermal stability [4-8]. Due to these advantages, their potential has been tested for the design and development of new sensors. These structures can generate polymeric films by electrooxidation, useful in various industrial purposes like anticorrosion protection or environmental monitoring. The ligand 2,6-bis((E)-2-(furan-2-yl) vinyl)-4-(5-

[1] PhD student, Dept. of Inorganic Chemistry, Physical Chemistry and Electrochemistry, University POLITEHNICA of Bucharest, Romania: e-mail: oana.enache18@yahoo.com
[2] PhD student, Dept. of Inorganic Chemistry, Physical Chemistry and Electrochemistry, University POLITEHNICA of Bucharest, Romania: e-mail: maticaovidiu@yahoo.co.uk
[3] PhD eng., Dept. of Inorganic Chemistry, Physical Chemistry and Electrochemistry, University POLITEHNICA of Bucharest, Romania: e-mail: m_bujduveanu@yahoo.com
[4] Professor, Doctoral School "Applied Chemistry and Materials Science", University POLITEHNICA of Bucharest, Romania, e-mail: em_ungureanu2000@yahoo.com
[5] Eng., Institute of Organic Chemistry C. D. Nenitzescu of Romanian Academy, Bucharest, Romania, e-mail: mihcris2012@yahoo.ro

isopropyl-3,8-dimethylazulen-1-yl) pyridine has been subject of electrochemical experiments using cyclic voltammetry (CV), rotating disk electrode voltammetry (RDE) and differential pulse voltammetry (DPV) [9, 10]. It has been used to build chemically modified electrodes (CMEs) for Pb^{2+} analysis, with good results (detection limit of 10^{-7} M) [11]. Starting from this premise, the present study focused on the investigation of 4-(azulen-1-yl)-2,6-bis((E)-2-(furan-2-yl)vinyl)pyridine (**L**) ligand (Fig. 1), to evaluate its sensory response for HM ions recognition. This azulene compound was previously synthetized and characterized by physical chemical methods [10]. In the present paper, the **L** was characterized by electrochemical methods, and the preparation of the poly**L** modified electrodes has been studied. The HMs recognition based on these modified electrodes has been tested.

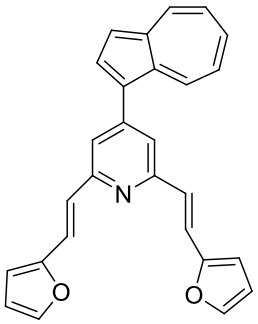

Fig. 1. Structure of 2,6-bis((E)-2-(furan-2-yl)vinyl)-4-(azulen-1-yl)pyridine

2. Experimental section

L has been synthetized in our laboratory as stated in previous paper [10]. Tetrabutylammonium perchlorate (TBAP), acetonitrile (CH_3CN), mercury (II) acetate (≥98%), cadmium nitrate tetrahydrate (≥98%), copper (II) acetate monohydrate (≥98%) and lead (II) nitrate (≥99.5%), all reagents purchased from Fluka were used as received to prepare the synthetic stock solutions (10^{-3} M) of HM ions. HMs non-aqueous solutions with different concentrations were prepared by successive dilution.

The electrochemical experiments were carried out on PGSTAT 302N AUTOLAB potentiostat coupled to a three-compartment cell. The working electrode was a glassy carbon disk (3 mm in diameter, from Metrohm). Before each determination, the electrode' surface was polished with diamond paste (0.25 μm) and cleaned with CH_3CN. The reference electrode was Ag/10 mM $AgNO_3$ in 0.1 M TBAP, CH_3CN. At the end of experiments performed in acetonitrile solution, the potentials were referred to the ferrocene/ferricinium redox couple (Fc/Fc^+) potential. The auxiliary electrode was a platinum wire. The experiments were performed at 25 ºC under argon atmosphere.

The cyclic voltammetry (CV) curves were recorded at scan rates between 0.05 and 1 V/s. The differential pulse voltammetry (DPV) curves were recorded at 0.01 V/s with a pulse height of 0.025 V, and a step time of 0.2 s. The rotating disk electrode voltammetry (RDE) experiments were performed at 0.01 V/s with rotation rates between 500 and 1500 rpm.

CMEs have been prepared from millimolar solutions of **L** in 0.1 M TBAP/CH_3CN by scanning or controlled potential electrolysis (CPE). Then, each modified electrode (**L**-CME) was washed with acetonitrile and introduced in 0.1 M acetate buffer solution (pH = 4.5), where it was equilibrated and overoxidized as previously described [11, 12]. The resulting electrodes were immersed for 15 min under stirring in synthetic solutions of HM ions. After that, the electrodes were taken out and cleaned with deionized water, then immersed in a cell containing 0.1 M acetate buffer solution (pH = 4.5). Here, they were polarized for 3 min at −1.2 V, and then their DPV curves were recorded between −1.2 V and +0.6 V.

3. Results and discussions

3.1 Electrochemical studies

The electrochemical behaviour of **L** on glassy carbon was studied in 0.1 M TBAP, CH_3CN. The curves showing the oxidation and reduction processes were recorded separately starting from the equilibrium potential to more positive or negative potentials, respectively. Their starting points are marked by arrows.

Study by CV and DPV

The electrochemical characterization of **L** was performed by CV at constant scan rate (0.1 V/s) in solutions with millimolar concentrations (0.5–2 mM) of **L** (Fig. 2), and in various potential scan domains (Fig. 3). CV curves for 1 mM **L** solution at different scan rates (0.05–1 V/s) are exhibited in Fig. 4.

To compare the values of currents for anodic and cathodic in oxidation (a1–a3) and reduction (c1–c3) processes of **L**, the cathodic CV currents were shown in absolute values in Fig. 2. The successive anodic and cathodic processes are denoted in the order in which they appear in the voltammograms. The curves for the supporting electrolyte were also recorded and they are drawn here with dotted lines. The CV curves are shown in parallel with voltammograms obtained by DPV to compare their peak potentials. It can be observed that DPV and CV currents for anodic and cathodic peaks increase with the concentration of **L** and at low **L** concentrations the dependences are linear.

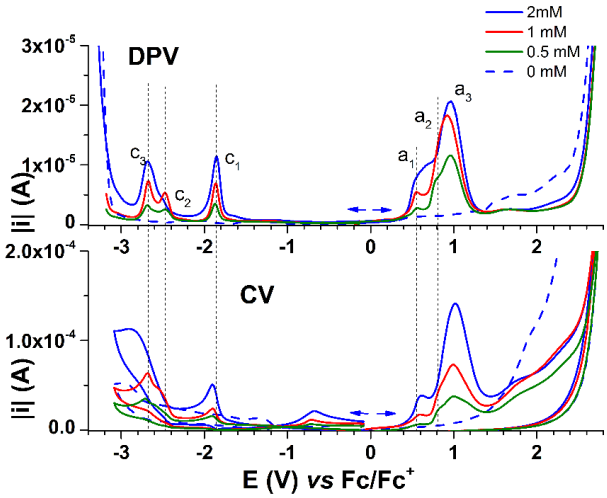

Fig. 2. DPV (0.01 V/s) and CV (0.1 V/s) curves (the currents are in absolute values) on glassy carbon for **L** in 0.1 M TBAP/ CH_3CN at different concentrations (mM): 0 (dotted blue line), 0.5 (green line), 1 (red line), 2 (blue line).

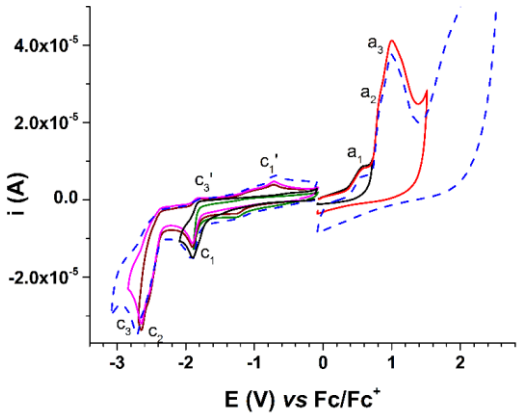

Fig. 3. Oxidation and reduction CV curves for curves for 1 mM **L** in 0.1 M TBAP/ CH_3CN solution at 0.1 V/s on different domains of potential scan.

Fig. 3 confirms the gradual appearance of the peaks with the extension of the scanning potential limit. Obviously, a1-a3, and c1-c3 processes are related to **L** which undergoes electron transfers (accepts or loses electrons). There are also small peaks due to other secondary processes such as oxygen reduction from residual water (at about -1.2 V on cathodic scan) or oxide formation (at about 1.4 V on anodic scan), as well as an overoxidation at some extent of the polymeric films generated during the scanning. The last one is more intense at lower monomer concentrations. This hypothesis is consistent with the more significant

decrease of the currents observed by us in the chrono-amperograms at higher anodic potentials (see below).

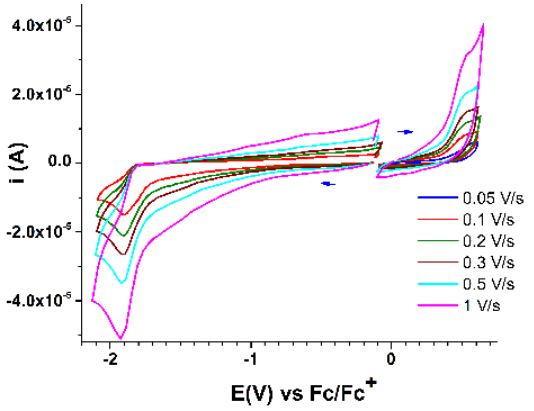

(A)

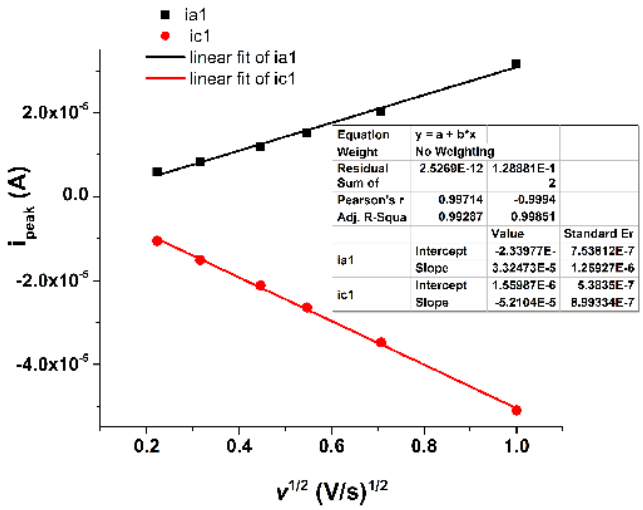

(B)

Fig. 4. CV voltammograms for oxidation and reduction processes at different scan rates for 1 mM **L** solution (A); linear dependences of the peak currents on the square root of the scan rate for (a1) and (c1) peaks recorded at 0.6 V and -1.80 V potentials, respectively (B).

Fig. 4 A shows clearly for (a1) and (c1) peaks that the currents increase with the increase of the scan rate. Linear dependences (Fig. 4 B) of the peak currents on the square root of the scan rate are noticed with absolute slopes of 3.32473×10^{-5} $A\cdot V^{-1/2}\cdot s^{1/2}$ for a1 peak and 5.2104×10^{-5} $A\cdot V^{-1/2}\cdot s^{1/2}$ for c1 peak, These slopes agree with a ratio of 2:1 between the number of electrons involved in the first oxidation and reduction processes. According to linear dependences of peak current on both concentration and square root of the scan rate it results that the the first electrochemical process of **L** (oxidation or reduction) is diffusion controlled.

The reversible character of each process was established from cyclic voltammograms obtained at different scan rates and domains, as well as from the RDE curves (see the next section) and is given in Table 1. Fig. 3 shows that c1 and c3 peaks, noticed in the cathodic scans on the CV curves on different potential domains are quasireversible from electrochemical point of view because these peaks have response peaks (c1' and c3') in the return sweeps. All other processes appear to be irreversible.

Table 1

Values od peak potentials (V vs. Fc/Fc^+) from CV and DPV curves for peaks attributed to anodic and cathodic processes of L, as well as their reversibility characteristics

Peak	CV	DPV	Process characteristics
a1	0.591	0.548	Irreversible
a2	0.837	0.804	Irreversible
a3	0.988	0.917	Irreversible
c1	-1.902	-1.862	Quasireversible
c2	-2.551	-2.476	Irreversible
c3	-2.687	-2.680	Quasireversible

Study by RDE

Fig. 5 presents two series of voltammgrams with rotating disc electrode (RDE) having as comparison the DPV curves (on top). One RDE example is for constant concentration of **L** (0.6 mM) in 0.1 M TBAP/CH_3CN obtained at different rotation rates (500–1500 rpm). The second one is for constant 1000 rpm rotation rate at **L** concentrations of 0, 0.6 and 1 mM. The cathodic currents are drawn in absolute values. In the first group of RDE curves an increase of first limiting current with rotation rate (rpm) for the processes in the cathodic domain (corresponding to the DPV peak c1) can be noticed. However, after the c2 process the order is reversed (the higher rotation rates the smaller the limiting currents), proving irreversibility of c2. Also, there is no regular behaviour of RDE waves for the processes in the anodic domain (corresponding to the DPV peaks a1-a3), where the waves almost overlap at different rotation rates. The shape of RDE curves in the anodic scan is certainly due to the formation of polymeric films that cover the electrode surface, and lead to the decrease of the currents to low values, probably close to the background.

RDE curves at different L concentrations, recorded in the bottom of Fig. 5, show that the cathodic waves confirm the two limiting currents in the c1 and c3 potential regions, as well as the overlapping of curves in the anodic sweep.

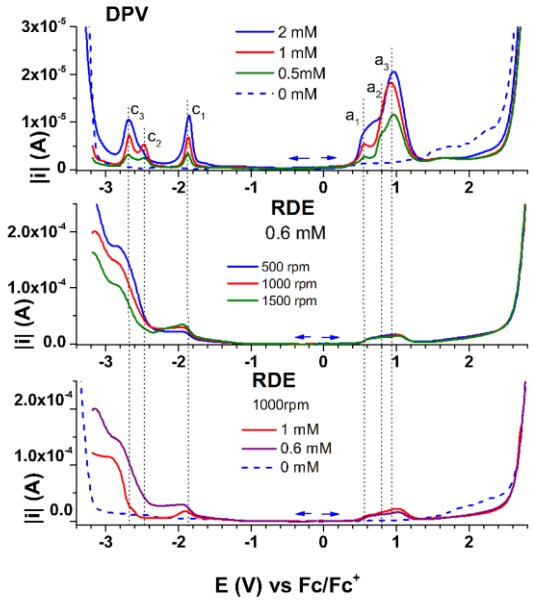

Fig. 5. Examples of RDE curves of oxidation and reduction of **L** on glassy carbon: for 0.6 mM **L** solution at different rotation rates (rpm) and for constant 1000 rpm rotation rate at various **L** concentrations in 0.1 M TBAP/ CH_3CN. In the top are presented, for comparison, the DPV (0.01 V/s) curves shown above in Fig. 2.

3.2. Formation of polyL films

Electrochemical immobilization of **L** on GC electrode has been carried out in millimolar solutions of **L** in 0.1 M TBAP/CH_3CN either by potential scanning, or by CPE at potentials in the region of **L** anodic processes (as seen in section 3.1). After preparation, the modified electrodes (**L**-CMEs) were cleaned with acetonitrile and transferred into ferrocene solutions in 0.1 M TBAP/CH_3CN to check the films formation by ferrocene redox assay probe.

Film formation by scanning

Fig. 6 shows the evolution of CV curves during successive scans in the domain of processes a1- a2 (Fig. 6A) and a3 (Fig. 6B), respectively. Except the cycle 1, the other voltammograms tend to overlap, reaching a steady state at cycle 10. The irreversibility of anodic oxidation of **L** during polymeric film preparation is clearly demonstrated. More detailed, if the sweep was up to 0.8 V the current initially decreases drastically during cycles 2-3, and after the 3rd cycle begins to increase in potential region of 0.7-0.8 V. This indicates an increase in the surface of the electrode after the third scan cycle. If the sweep was up to 1.6 V (B) the currents decrease continuously during cycling which indicates the coating of the electrode with non-conductive films.

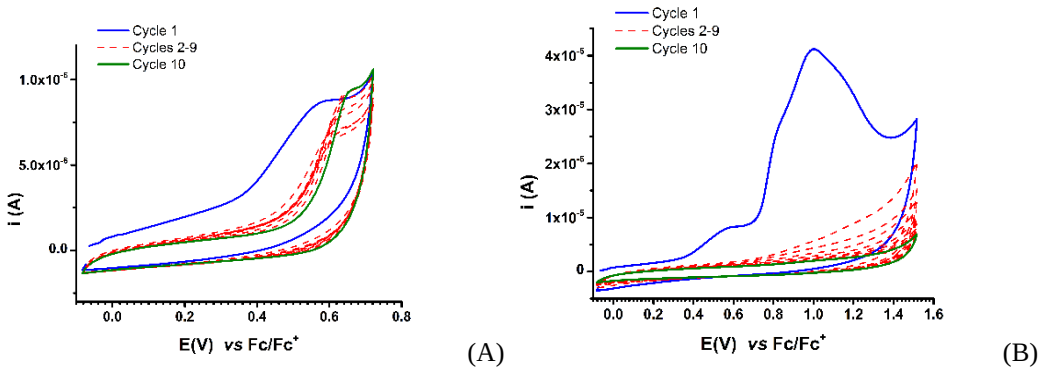

Fig. 6. Successive ten anodic voltammograms (0.1 V/s) in 1 mM solution of **L** on different domains of potential: up to 0.8 V (A) and extending the potential up to 1.6 V (B)

The comparative recorded cathodic CV curves in ferrocene (Fc) solution of the obtained **L**-CMEs and of the bare electrode (Fig. 7) also confirm the formation of thin films.

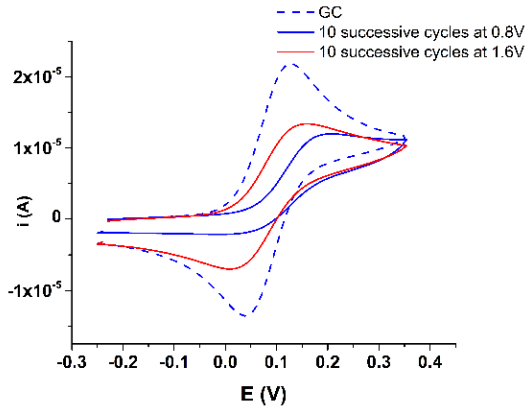

Fig. 7. CV curves (0.1 Vs^{-1}) recorded after the transfer of **L**-CMEs in 1 mM ferrocene solution in 0.1 M TBAP/ CH_3CN compared to those recorded on bare electrode (dashed line). **L**-CME films were prepared during 10 cycles in 1 mM **L** solution on domains of potential up to 0.8 V and 1.6 V (see Fig.6).

The polymeric film on modified electrodes prepared by successive cycling behaves almost reversible, in fact quasireversible, because the ferrocene signals as anodic and cathodic peak potentials are shifted, and the peak currents are very much diminished.

Films formation by CPE

Electrochemical immobilization of **L** on GC electrode has also performed in **L** solutions of different concentrations in 0.1 M TBAP/CH_3CN by CPE. During film formation we recorded the current transients by polarizing the electrode at different imposed potentials keeping constant the electrical charge. The

corresponding chronoamperograms are given in Fig. 8. By applying this technique, reproducible **L**-CMEs have been prepared as blue films on the electrode surface as blue films. When testing the modified electrodes obtained by CPE by ferrocene redox probe, the obtained CV curves (Fig. 9) showed important changes in comparison with that recorded for the bare electrode (dashed line).

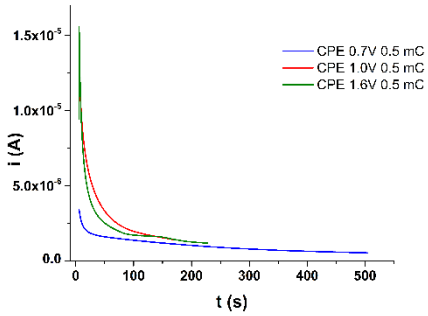

Fig. 8. Chronoamperograms during the preparation of **L**-CMEs in 0.5 mM solution of **L** in 0.1 M TBAP, CH_3CN by CPE at different imposed potentials using 0.5 mC electrical charge.

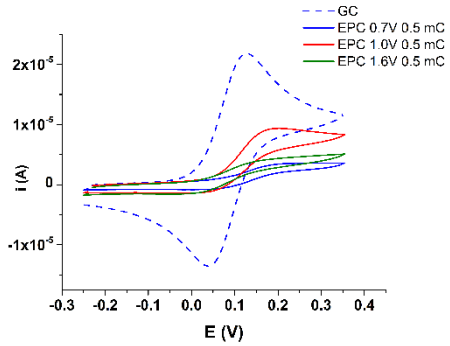

Fig. 9. CV curves (0.1 V s-1) recorded after the transfer of the **L**-CMEs prepared by CPE (Fig.9) in ferrocene solution (1 mM) in 0.1M TBAP/ CH_3CN compared to those recorded on bare electrode

3.3. Heavy metal species recognition experiments using polyL films

For HM ions recognition, **L**-CMEs obtained by CPE in 0.5 mM **L** in 0.1 M TBAP/CH_3CN were tested by the procedure already described [12]. After preparation and careful cleaning with acetonitrile, the modified electrodes were introduced in acetate buffer (0.1 M) at pH 4.5 and cycled for equilibration and overoxidation. After that, they were immersed in synthetic solutions in water containing a mixture of HM ions (Cd, Pb, Cu and Hg dissolved species), simulating polluted media. Then they were introduced in acetate buffer (pH 4.5) and polarized at −1.2 V for 3 min. Finally, the potential was linearly swept in anodic scans using DPV technique (Fig. 10A).

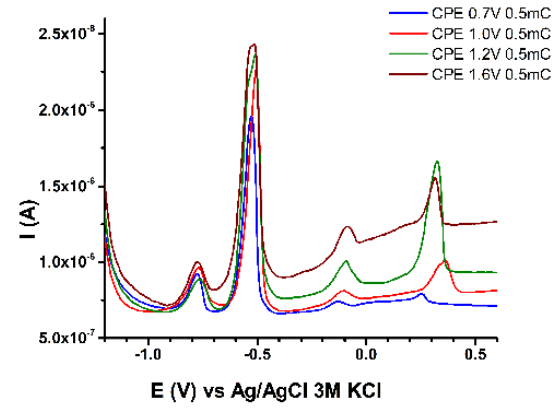

(A)

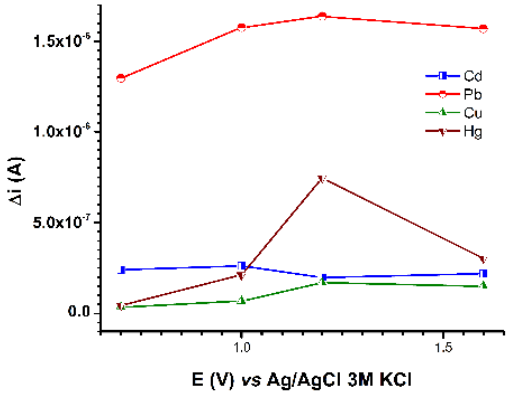

(B)

Fig. 10. Stripping DPV curves showing the influence of applied CPE potential (0.7-1.6 V) at constant electrical charge (0.5 mC) on HM peaks (A); The dependence of peak current difference (Δi), starting from DPV peak current for bare electrode, on imposed CPE potential for all investigated HM species (each in concentration of 10^{-5} M)

Stripping peaks for Cd, Pb, Cu and Hg ions (each having a 10^{-5} M concentration) were noticed at the potentials of −0.813 V, −0.565 V, −0.112 V, and +0.282 V, respectively. For each investigated HM ion, the DPV curves in the tested accumulation solutions showed the corresponding stripping peak currents which are higher than for bare electrode (non-covered glassy carbon). This behaviour indicates that these ions have been retained in the electrogenerated films, ensuring the immobilization into **L** complexing units in different percentages. Fig. 10B shows the peak current difference (Δi), starting from DPV peak current for each imposed anodic potential for stripping. By keeping a constant applied potential at stripping (1.6 V) the heights of signal for HM ions are very different in the DPV curves obtained on **L**-CMEs (Fig. 11).

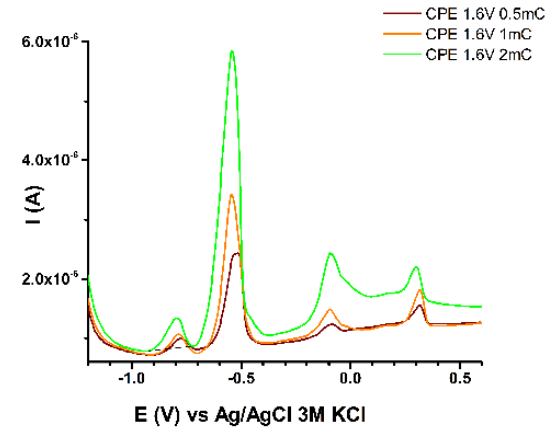

(A)

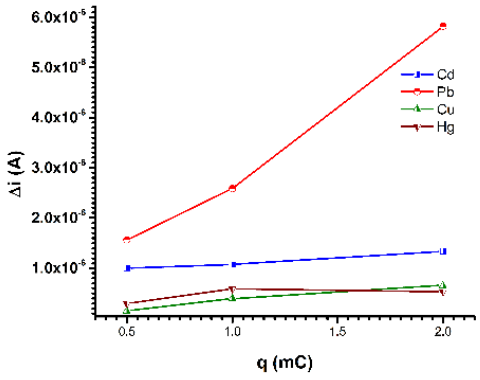

(B)

Fig. 11. Influence of the charge used in constant CPE (1.6 V) for preparation of modified electrode on HM peaks in the stripping DPV (A). Dependence of DPV peak current difference (Δi), starting from DPV peak current for bare electrode on CPE charge (B) for all investigated HM species (each in 10^{-5}M concentration)

This figure shows a selective complexation for Pb, which has the highest signal at −0.565 V. Certainly, the peak for Pb(II) is influenced by the film thickness which is conditioned by the electropolymerization charge.

4. Conclusions

This study relates the characterization of 2,6-bis((E)-2-(furan-2-yl) vinyl)-4-(azulen-1-yl) pyridine by three electrochemical techniques: cyclic voltammetry, pulse-differential voltammetry, and rotating disk electrode voltammetry. The electrochemical study was performed in to establish the main features for subsequent applications, such as films formation during preparation of modified

electrodes or heavy metal ions sensing. One of the results shows that the estimated detection limit of Pb species is less than 10^{-8} M.

Acknowledgements

This research was funded by Romanian National Authority for Scientific Research, UEFISCDI, under grant PN-III-P2-2.1-PED-2019-0730, contract no. 293PED/2020.

R E F E R E N C E S

[1]. *E.-M. Ungureanu, A.C. Razus, L. Birzan, M.-S. Cretu, G.-O. Buica*, "Electrochemical study of azo–azulene compounds", in Electrochimica Acta, **vol. 53**, 2008, pp. 7089-7099

[2]. *E. Diacu, G.-O. Buica, I. Chilibon, L. Birzan, G.-L. Arnold, E.-M. Ungureanu*, "Chemically Modified Electrodes Based on 5- (Azulen-1-yl) methylene)-2-thioxothiazolidin-4-one", in Journal of Solution Chemistry, **vol. 45**(11), 2016, pp. 1588–1597

[3]. *M.D. Pop, V. Anastasoaie, M.A. Popescu, A. Oprisanu, E.M. Ungureanu, M. Cristea*, "New Azulene Modified Electrodes for Heavy Metal Sensing", in Revista de Chimie, **vol. 68**(9), 2017, pp. 2172-2175

[4]. *N.R. Honesty, G. Kardaş, A.A. Gewirth*, "Investigating Rhodanine film formation on roughened Cu surfaces with electrochemical impedance spectroscopy and surface-enhanced Raman scattering spectroscopy", in Corrosion Science, **vol. 83**, 2014, pp. 59–66

[5]. *S. Nho, D.H. Kim, S. Park, H.N. Tran, B. Lim, S. Cho*, "Carbazole and rhodanine based donor molecule with improved processability for high performance organic photovoltaics", in Dyes and Pigments, **vol. 151**, 2018, pp. 272–278

[6]. *J. Baell, M.A. Walters*, "Chemistry: Chemical con artists foil drug discovery", in Nature, **vol. 513**(7519), 2014, pp. 481–483

[7]. *J.L. Dahlin, M.A. Walters*, "The essential roles of chemistry in high-throughput screening triage", in Future Medicinal Chemistry, **vol. 6**(11), 2014, pp. 1265–1290

[8]. *G. Kardaş, R. Solmaz,* "Electrochemical synthesis and characterization of a new conducting polymer: Polyrhodanine", in Applied Surface Science, **vol. 253**(7), 2007, pp. 3402–3407

[9]. *A.C. Razus, L. Birzan, C. Pavel, O. Lehadus, A. Corbu, F. Chiraleu, C. Enache*, "Azulene--substituted pyridines and pyridinium salts. Synthesis and structure. 1. Azulene-substituted pyridines", in Journal of Heterocyclic Chemistry, **vol. 44**(1), 2007, pp. 245-250

[10]. *L. Birzan, M. Cristea, C.C. Draghici, V. Tecuceanu, A. Hanganu, E.M. Ungureanu, A.C. Razus*, "4-(Azulen-1-yl) six-membered heteroaromatics substituted in 2- and 6- positions with 2-(2-furyl) vinyl, 2-(2-thienyl) vinyl or 2-(3-thienyl) vinyl moieties", in Tetrahedron, **vol.73**, 2017, pp. 2488-2500

[11]. *L.-B. Enache, V. Anăstăsoaie, C. Lete, A.G. Brotea, O.-T. Matica, C.-A. Amarandei, J. Brandel, E.-M. Ungureanu, M. Enachescu*, "Polyazulene-Based Materials for Heavy Metal Ion Detection. 3. (E)-5-((6-t-Butyl-4,8-dimethylazulen-1-yl) diazenyl)-1H-tetrazole-Based Modified Electrodes", in Symmetry, **vol. 13**(9), 2021, pp. 1642

[12]. *E.-M. Ungureanu, V. Anăstăsoaie, M.-R. Bujduveanu, A.G. Brotea, R. Isopescu, G. Stanciu*, "Polyazulene Based Materials for Heavy Metal Ions Detection. 4. Search for Conditions for Thiophen-Vinyl-Pyridine-Azulene Based CMEs Preparation" in Symmetry, **vol. 14**, 2022, pp. 225.